

# An Experimental Study on the Behavior of Reinforced UHPFRC Ties Under Serviceability Conditions

*Un Estudio Experimental Sobre el Comportamiento de Tirantes armados de HMAR bajo Condiciones de Servicio*

Majid Khorami\*<sup>c, d</sup>, Juan Navarro-Gregori<sup>a</sup> & Pedro Serna Ros<sup>b</sup>

<sup>a</sup> Associate Professor, Instituto de Ciencia y Tecnología del Hormigón (ICITECH), Universitat Politècnica de València

<sup>b</sup> Professor, Instituto de Ciencia y Tecnología del Hormigón (ICITECH), Universitat Politècnica de València

<sup>c</sup> Assistant Professor, Facultad de Arquitectura y Urbanismo, Universidad UTE, Quito, Ecuador

<sup>d</sup> PhD candidate, Instituto de Ciencia y Tecnología del Hormigón (ICITECH), Universitat Politècnica de València

## RESUMEN

El estudio del comportamiento a tracción de los elementos armados de Hormigón de Muy Alto Rendimiento (R-HMAR) es un aspecto esencial para la verificación de los **Estados Límite de Servicio (ELS)** de fisuración y deformaciones. En este trabajo se presentan los resultados de una campaña experimental de tirantes R-HMAR con diferentes matrices de hormigón y cuantías de armado. Se comparan las propiedades mecánicas a tracción obtenidas en los elementos armados con las obtenidas de probetas de flexotracción sin armar. El análisis de resultados revela la importancia de la retracción en la respuesta de los elementos R-HMAR.

## ABSTRACT

The study of tensile behaviour of Reinforced Ultra-High Performance Fibre-Reinforced Concrete elements (R-UHPFRC) is an essential aspect for the verification of **Serviceability Limit State (SLS)** crack and deflection control. This work presents the results of an experimental campaign of R- UHPFRC ties with different concrete matrices and reinforcement ratios. The tensile mechanical properties obtained in the reinforced elements are compared with those obtained from bending tests without reinforcement. The analysis of results reveals the importance of shrinkage in the response of the R-UHPFRC elements.

**PALABRAS CLAVE:** ensayo de flexión, servicio, tirante, R-HMAR

**KEYWORDS:** bending test, serviceability, tie, UHPFRC

## 1. Introduction

The fundamental requirements associated with serviceability are functionality, user comfort, and appearance. However, these requirements cannot be verified directly; thus, performance criteria, such as deflection control, vibration control, and cracking control, are defined to

meet these requirements[1]. In many structural design situations, practically in systems such as house and medium-sized commercial buildings, acceptable structure performance is seldom defined by ultimate limit states. Rather, it is controlled by serviceability requirements.

**Table 1. Mix proportions of UHPFRC for concrete type C1 and C2-unit content (kg/m<sup>3</sup>)**

Medium Sand 0.6–1.2 mm	Fine Sand 0.5 mm	Silica Flour U-S500	Silica fume (Elkem Microsilica, grade 940)	Cement	Superplasticizer	Water	Fiber
565	302	225	175	800	30	160	Concrete type (C1) 160
							Concrete type (C2) 80

Serviceability calculation is complicated because of the cracking phenomenon, tension stiffening effect, shrinkage, and creep effects. Cracking control in reinforcement concrete structures is generally achieved by limiting the stress increment in steel reinforcement to an appropriately low value. Many concrete code designs specify maximum steel reinforcement stress after cracking and maximum crack width. The design serviceability aspects for Reinforced Ultra-High Performance Fiber-reinforced Concrete (R-UHPFRC) are not included in CEB-FIP Model Code 2010 (MC10)[2] and are poorly considered in UHPFRC codes or recommendations such as French standard and recommendations NF P18-470, AFGC [3] Japanese standard and guideline JSCE concrete Committee[4], and Switzerland technical notebook for SIA 2052[5]. Thus, research in this area is steadily growing.

To predict the structural behavior of UHPFRC concrete members, a simple model is required to represent the tensile behavior of the UHPFRC material. An inverse analysis method can be used to derive the tensile material properties from load-deflection response obtained from four-point bending tests (4PBTs)[6,7]. A new inverse analysis method based on deflection to curvature transformation to determine the tensile properties of UHPFRC was proposed in the previous research by authors[8,9]. In this research an uniaxial tensile R-UHPFRC tie test was conducted.

The experimental program included in this study consisted of nine series of prismatic tie elements with varying rebar diameters and cross-section dimensions and two different types of concrete in terms of fiber content. Finally,

tension stiffening response under service loads was obtained, and compared with the tensile properties obtained from bending tests.

## 2. Experimental Program

### 2.1 Mixture proportion and mechanical properties of UHPFRC

Parameters related to fibers, such as type, content, and fiber length, affect the properties of UHPFRC. Therefore, the influence of each factor on the mix design of concrete must be considered. This study focuses on the influence of fiber content on the tensile behavior under SLS loads. However, the influences of reinforcement ratio and section dimensions are also presented to make a comprehensive conclusion.

The test program was conducted with two types of concrete mixtures that only vary in fiber content. Fiber dosages of 160 and 80 kg/m<sup>3</sup> were used in this study. The base of mixture proportion and aggregate characteristics were as previous research by authors[10]. The main components of the mixtures were cement, silica fume, silica flour, fine sand, and medium sand. The mix proportion is described in Table 1. The cement type was type I-sulfate resistant cement, and its compression strength was 42.5 MPa on the 28th day according to the supplier. The silica sand specific gravity was 2.61 g/cm<sup>3</sup>, and two size ranges were used. The fine and medium sand were 0.5 and 0.6–1.2 mm in size, respectively.

With its small grain size, silica fume fills the space in between cement grain and improves

**Table 2. Description of test specimens.**

Concrete Type and Fiber Content		Section Size	Rebar Size (mm)	$\rho$ (%)	Cover (mm)	Material Properties	
C1 ( $V_f = 160 \text{ kg/m}^3$ )	C2 ( $V_f = 80 \text{ kg/m}^3$ )					Compression Strength (MPa)	
Specimen Id	Specimen Id					$f'_c, C1$	$f'_c, C2$
d10F160S6-1-b3	d10F80S6-1-b3	60×60 mm <sup>2</sup>	Ø10	2.18	25	151.32	141.38
d10F160S6-2-b2	d10F80S6-2-b3					151.32	141.38
d10F160S6-3-b5	d10F80S6-3-b4*					150.16	-
d12F160S6-1-b6	d12F80S6-1-b5		Ø12	3.13	24	154.41	147.12
d12F160S6-2-b6	d12F80S6-2-b5					154.41	147.12
d12F160S6-3-b2	d12F80S6-3-b6*					150.16	-
d16F160S6-1-b3*	d16F80S6-1-b6*		Ø16	5.58	22	-	-
d16F160S6-2-b3*	d16F80S6-2-b6*					-	-
d16F160S6-3-b4*	d16F80S6-3-b6*					-	-
d10F160S8-1-b6	d10F80S8-1-b6*	80×80 mm <sup>2</sup>	Ø10	1.23	35	150.16	-
d10F160S8-2-b3	d10F80S8-2-b6*					148.43	-
d10F160S8-3-b3	d10F80S8-3-b5*					148.43	-
d12F160S8-1-b2	d12F80S8-1-b4		Ø12	1.77	34	124.8	124.89
d12F160S8-2-b5	d12F80S8-2-b4					150.16	124.89
d12F160S8-3-b3	d12F80S8-3-b4					148.43	124.89
d16F160S8-1-b5	d16F80S8-1-b6*		Ø16	3.14	32	151.32	-
d16F160S8-2-b4	d16F80S8-2-b6*					149.39	-
d16F160S8-3-b4	d16F80S8-3-b5*					149.39	-
d10F160S10-1-b1	d10F80S10-1-b3	100×100 mm <sup>2</sup>	Ø10	0.79	45	166.67	148.25
d10F160S10-2-b2	d10F80S10-2-b5					150.16	148.25
d10F160S10-3-b1*	d10F80S10-3-b3					-	147.12
d12F160S10-1-b1	d12F80S10-1-b1		Ø12	1.13	44	151.32	148.25
d12F160S10-2-b2	d12F80S10-2-b1					166.67	148.25
d12F160S10-3-b1	d12F80S10-3-b2					166.67	166.67
d16F160S10-1-b1	d16F80S10-1-b1*		Ø16	2.01	42	151.32	-
d16F160S10-2-b2	d16F80S10-2-b1*					166.67	-
d16F160S10-3-b3	d16F80S10-3-b6*					166.67	-

\* These specimens are not yet tested.

The IDs of the specimens were as follows dxx Fxx Sxx-#-b#, where (dxx) is the rebar diameter in millimeters, (Fxx) is the fibre content in kg/m<sup>3</sup>, (Sxx) is the cross-section size in cm, (#) is the number of specimens of each group, and (b#) is the concrete batch number.

the density and reduces the porosity of UHPFRC [11]. Small steel fibers with a diameter length of 13 mm, and tensile strength beyond 2000 MPa were used in this study.

A standard horizontal pan mixer was used. First, the dry ingredients silica sand, cement, silica flour, and silica fume were mixed for approximately 1 min. Water and superplasticizer were then added, and the materials were further mixed for 10 min until a homogeneous mixture was obtained and the dry powder mix was transformed into a wet paste concrete. The small straight steel fibers were

slowly spread by hand to the wet concrete paste in the mixer. The concrete was further mixed for 5 min to ensure the proper dispersion of fibers. Finally, the fresh UHPFRC material was cast into prismatic and cube standard specimen molds. Given that a superplasticizer was used, the concrete did not need to undergo vibration to remove entrapped air in the specimen molds. Specimens from both mixes were cured for 24 h at laboratory temperature ( $25 \pm 2$  °C) before demolding. Thereafter, all of the specimens were placed in a high-humidity curing room at 95%

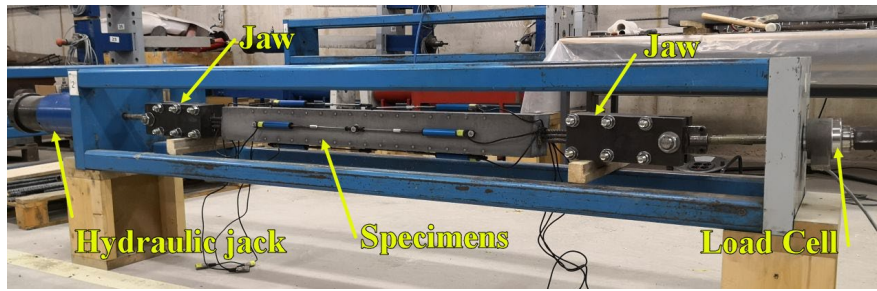


Figure 1. Test setup parts and installed specimen

relative humidity and temperature of  $T = 20 \pm 2$  °C until 2 or 3 days before testing.

Four cubic specimens ( $100 \text{ mm}^3$ ) were used to evaluate the average UHPFRC compression strength. The values were 152.97 and 142.95 MPa for concrete types C1 and C2, and the average Young's modulus values obtained by using two cylindrical specimens  $150 \times 300 \text{ mm}^2$  were 48.5 and 46.5 GPa. The nominal yield stress of steel rebars was  $f_y \approx 500$  MPa and the modulus of elasticity was  $E_s = 200$  GPa. The specimen description and concrete strength for each concrete type and concrete batch are presented in Table 2.

## 2.2 Specimen preparation and experimental test setup

The specimens were made in prismatic shape with square cross-section with a length of 1000 mm. In this experimental study, three different cross-section sizes (60, 80, and 100 mm) and three steel reinforcement rebar diameters ( $\text{Ø}10$ ,  $\text{Ø}12$ , and  $\text{Ø}16$ ) were used to consider the reinforcement ratio effect on the R-UHPFRC behavior. Three specimens were cast for every section and rebar size group.

Notably, not all of the specimens have been tested due to time limitations, large number of specimens, and challenges in direct tensile testing in the laboratory. Thus, this paper only discusses the test results obtained so far. Table 2 provides the main characteristics and details of R-UHPFRC ties.

## 2.3 Test procedure

A novel test system for performing the tensile tie test has been proposed [10]. The proposed test system and method were suitable for the experimental test of R-UHPFRC ties under SLS loading. Two pieces of steel jaw were employed for applying the tension load to the 24 cm-length extended bars at each end of the specimen. The specimens were tested under manual displacement control at a rate of approximately 0.5 mm/min. Eight displacement transducers (DTs) were installed on the surfaces of the specimens to record element elongation during the test and capture any bending applied to the specimen due to unforeseen load eccentricities. The 35 cm-long DTs were used and attached from the center of specimens through at extremes. The average value of deformations recorded by DTs was used for rebar deformation by assuming that surface deformations of concrete with steel rebar reinforcement were equal. The main steel test frame, hydraulic jack, and installed specimen are shown in Fig. 1. A load cell was used to measure force values.

## 3. Tensile behavior of R-UHPFRC

### 3.1 Tensile response

The direct tensile behavior of all specimens with concrete types C1 and C2 is shown in Fig. 2a and 2.b. Each curve represents the average result (average of the tensile stress values) of three

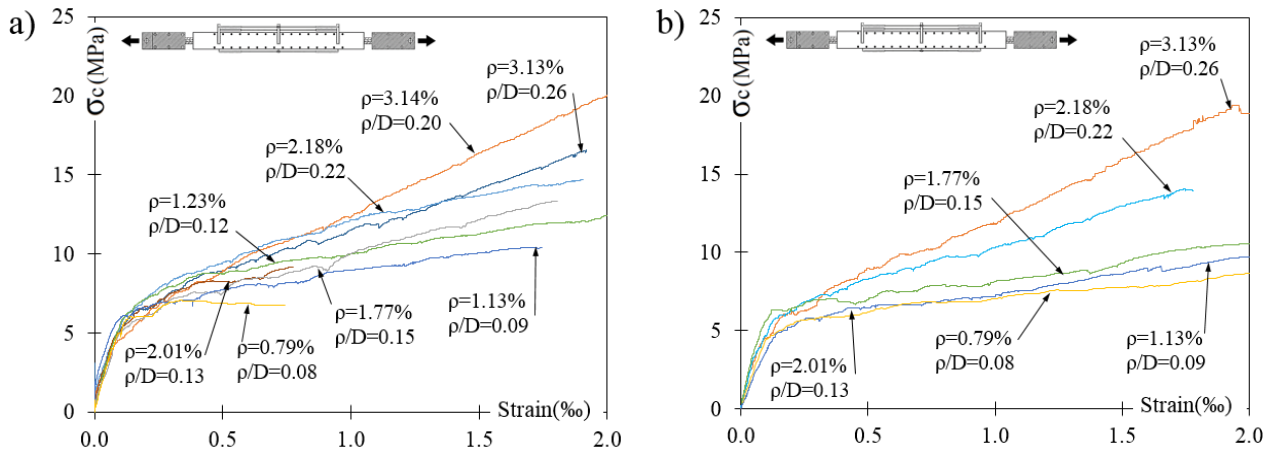


Figure 2. Tensile responses of reinforced UHPFRC: a) ties with concrete type C1 and b) ties with concrete type C2

specimens tested with same cross-section size and rebar diameter under axial tensile load (the average values were calculated from three specimens with identical cross-section and rebar diameter). Stress is the nominal stress obtained by uniaxial tensile force divided by concrete net-area. Note that these curves were labelled with reinforcement ratio ( $\rho=A_s/A_c$ ) and ( $\rho/D$ ), where ( $D$ ) is the rebar diameter.

### 3.2 Tension stiffening response

The cracked concrete member can carry tension between cracks due to the bond behavior of the reinforcing bar. This ability is called tension stiffening effect, which increases member stiffness before reinforcement yields[11]. This change of stiffness affects deflection and crack widths under service loads. In UHPFRC members, fibers carry remarkable tensile forces at a crack and effectively increase tension stiffening. Thus, tension stiffening effect is an essential parameter in structural elements designed under SLS conditions because this effect controls deflections, crack width, and crack spacing. The tension stiffening response for the R-UHPFRC tensile ties of specimens is presented in Figs. 3a and 3b.

The tension stiffening behavior for RC and FRC includes a descending branch after first cracking. However, this phenomenon is not

observed in the R-UHPFRC tensile members tested in this study, and the tension stiffening behavior remains near horizontal with a constant value. This result may be due to high bond-slip strength between the reinforcement and matrix of UHPFRC and the large number of microcracks along the entire length of the member, unlike localized cracks that typically occur in RC or FRC tie elements. Notably, microcracking was observed in all specimens during the test in the high rate of tensile strain before crack localization occurred.

## 4. UHPFRC tensile behavior characterization

### 4.1 Inverse analysis of four-point bending test results

The tensile stress-strain response of UHPFRC is a fundamental constitutive property of this material, which is one of the most essential aspects of serviceability design and prediction of the structural behavior. An inverse analysis method based on load–curvature method has been proposed and validated by the authors to determine the tensile properties of UHPFRC[8].

In order to validate and compare the tension contribution of UHPFRC (tension

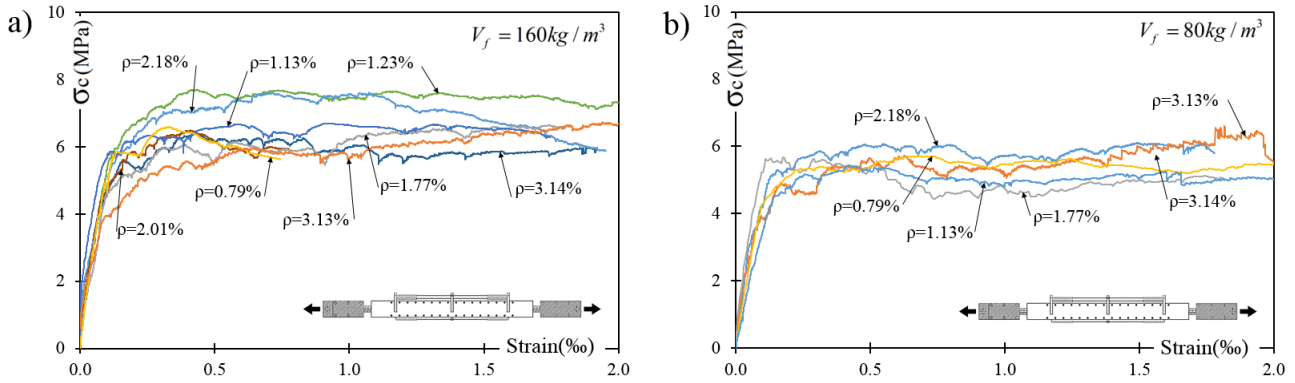


Fig. 3. Tension stiffening response of a) ties with concrete type C1 and b) ties with concrete type C2.

stiffening response) obtained by the R-UHPFRC tie test with inverse analysis method results, several four-point bending tests (4PBTs) were carried out. **Two prismatic specimens** ( $500 \times 100 \times 100 \text{ mm}^3$ ) were cast for each concrete batch and tested with flexural loading, and inverse analysis was applied to the results of each bending test. By inverse analysis method the parameters to define the constitutive UHPFRC behavior it can be obtained, which they are: cracking strength ( $f_t$ ), ultimate tensile strength ( $f_{t,u}$ ) and its corresponding strain ( $\varepsilon_{t,u}$ ), the crack opening at the change of slope ( $w_d$ ), the crack opening at zero stress ( $w_c$ ), and the elastic modulus ( $E$ ). (see Fig. 4).

Table 3 present the parameters to define the ( $\sigma - \varepsilon$ ) constitutive relationship according to the bending tests.

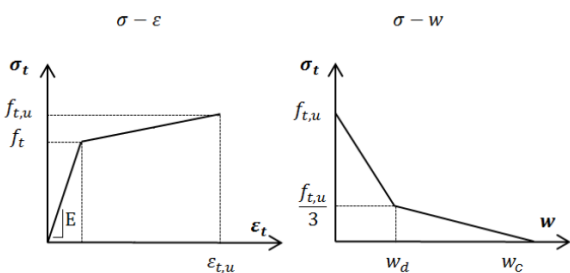


Figure 4. Assumed constitutive relationship for UHPFRC[12].



## 4.2 Comparison with experimental results

The tension stiffening response obtained from R-UHPFRC ties and the one obtained from the

proposed constitutive inverse analysis are presented in Figs. 5a and 5b for two types of tensile ties. The average bending test results are greater than the tension stiffening response obtained from the ties, even for the minimum obtained value. This discrepancy between the uniaxial tensile tie test results and the constitutive model can be due to several aspects such as fiber orientation, undesired internal bending rotations in the ties, or most probably due to the shrinkage effect. Bischoff [13] reported that the member response of RC specimens drops as shrinkage increases and resulting a lower cracking load and less apparent tension stiffening. The same phenomenon can occur for R-UHPFRC tensile tie elements. Shrinkage of concrete leads to an initial shortening of the R-UHPFRC member as indicated in Fig. 6, and causes a reduction in the cracking load. Shrinkage effect is an important parameter of analysis of the member response and the neglect of this effect leads to a perceived reduction in the cracking strength of the concrete and increase the reinforcing ratio in the design process[13].

The shrinkage of UHPFRC induces a negative pre-strain in the steel reinforcement ( $\varepsilon_{s,sh}$ ), which generates a negative stress (compression). Thus, the equivalent force to modify the origin of the load-deformation curve can be calculated by  $E_s A_s \varepsilon_{s,sh}$ . The pre-strain caused by shrinkage might significantly affect on tension stiffening, where the free shrinkage value

**Table 3. Constitutive Relationship Parameters for each concrete batch**

Concrete Type	Concrete batch number	Specimens	Constitutive Relationship Parameters				Modulus of elasticity of UHPFRC at 28 days (GPa)	
			$f_t$ (MPa)	$\varepsilon_{t,el}$ (‰)	$f_{t,u}$ (MPa)	$\varepsilon_{t,u}$ (‰)		
		A	11.66	0.22	11.12	5.79	48.4	
		B	8.94	0.18	8.03	4.40		
		A	8.05	0.16	6.77	2.09		
		B	7.77	0.14	6.27	2.14		
		A	10.43	0.19	8.90	4.49		
		B	9.49	0.17	8.40	4.43		
		A	8.89	0.17	7.91	4.47	48.1	
		B	8.79	0.17	7.97	1.54		
		B	10.42	0.20	9.95	3.57		
		C	10.45	0.22	10.42	4.71	48.1	
		Minimum result value		7.77	0.14	6.27		2.14
		Average result value		9.49	0.17	8.40		4.43
		1	A	6.10	0.10	4.37	3.32	46.3
			B	7.58	0.13	4.69	2.94	
			A	7.44	0.12	4.27	2.9	
B			7.35	0.13	4.13	2.81		
A			9.27	0.13	6.03	3.61		
B			7.83	0.14	5.10	3.18		
		A	8.06	0.15	7.22	2.60	46.5	
		B	9.15	0.16	9.05	2.83		
		B	8.11	0.12	5.46	4.35		
		A	8.06	0.16	5.97	4.80	46.6	
		A	8.11	0.12	5.46	4.35		
		B	8.06	0.16	5.97	4.80		
		A	8.54	0.18	4.61	2.24	45.9	
		B	8.72	0.15	4.44	1.24		
		Minimum result value		6.10	0.10	4.37		3.32
	Average result value		8.11	0.12	5.46	4.35		
	Maximum result value		9.27	0.13	6.03	3.61		

**Table 4. Tensile shrinkage strain and stress**

t (Concrete age)	$\varepsilon_{us}(t)$ ‰	$\sigma_{e,sh}$ (MPa)								
		Section 60x60 mm			Section 80x80 mm			Section 100x100 mm		
		Ø 10 (mm)	Ø 12 (mm)	Ø 16 (mm)	Ø 10 (mm)	Ø12 (mm)	Ø16 (mm)	Ø 10 (mm)	Ø12 (mm)	Ø 16 (mm)
Min = 37 days	0.53	2.16	3.02	-	1.25	1.77	3.02	1.01	1.43	2.46
Max = 198 days	0.67	2.73	3.82	-	1.58	2.24	3.82	1.28	1.81	3.12
Avg = 92 days	0.62	2.51	3.52	-	1.46	2.06	3.52	1.17	1.67	2.87

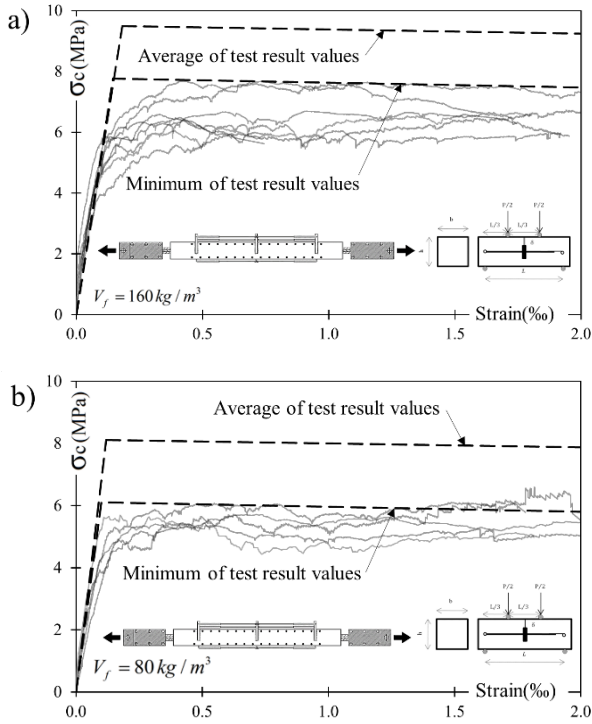


**Figure 5. Comparison between tension stiffening response and proposed constitutive model a) ties with concrete type C1 and b) ties with concrete type C2.**

can be estimated for UHPFRC using the following equation proposed by fprSIA 2052[5]:

$$\varepsilon_{Us}(t) = \varepsilon_{Us\infty} \cdot e^{\frac{c}{\sqrt{t+d}}} \quad (1)$$

The coefficients (c) and (d) are coefficients for setting the shrinkage model of UHPFRC. The proposed values of the coefficients by fprSIA 2052[5] are:  $c = -2.48$  and  $d = -0.86$ , and the age of concrete (t) is expressed in days. The fprSIA 2052[5] admits that the maximum value for shrinkage of UHPFRC is  $\varepsilon_{Us\infty} = 0.6 - 0.8\%$ . Due to a large number of specimens and the time required to complete the experimental program, the minimum and maximum age of specimens were 37 and 198 days, respectively. The shrinkage strain ( $\varepsilon_{Us}(t)$ ) and the corresponding concrete stress ( $\sigma_{c,sh}$ ) are provided in Table 4. The average Young's modulus values obtained by using  $150 \times 300 \text{ mm}^2$  cylindrical specimens were 48.53 and 46.49 GPa, respectively, and the value 47 GPa was used for calculating the shrinkage stress for both types of concrete.

This result leads to modify the tension stiffening response diagram (see Fig. 6) and adjusting the origin with the approximate range value 1.01 to 3.82 MPa depending on the concrete age, section size, rebar diameter, and Young's modulus values for each specimen. Consequently, the existing discrepancy between the constitutive model and tension stiffening response will modify with the shrinkage effect.

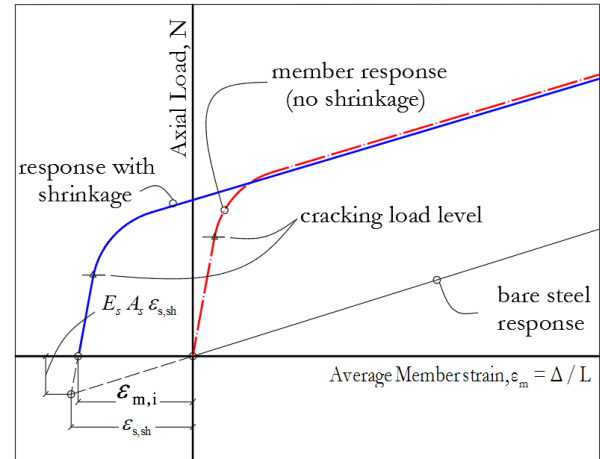


**Figure 6. Typical tensile R-UHPFRC tie behavior and the effect of shrinkage on member response**

## 5. Conclusions

The concrete tension contribution (tension stiffening response) obtained by the uniaxial R-UHPFRC tensile tie test was compared with the material characteristic properties of UHPFRC based on the proposed inverse analysis method. Nine series of ties and two types of concrete were developed to study the behavior of reinforced UHPFRC ties under serviceability conditions, and the shrinkage effect was evaluated theoretically. The shrinkage stresses were varied between 1.25 and 3.82 MPa depending on section size, rebar diameter, and age of concrete. This discrepancy between the uniaxial tensile tie test results and the characteristic properties obtained by the constitutive model indicates that it is necessary to incorporate the shrinkage effect in tension stiffening behavior of R-UHPFRC elements under serviceability conditions.



## Acknowledgments.

This study forms a part of the project BIA2016-78460-C3-1-R supported by the State Research Agency of Spain.

## References

- [1] D. Honfi, Design for Serviceability-A probabilistic approach, Lund University 2013.
- [2] J.C. Walraven, Model Code 2010-Final draft: Volume 1, fib Fédération internationale du béton 2012.
- [3] S. AFGC, Bétons fibrés à ultra-hautes performances—Recommandations provisoires, AFGC, France (2002).
- [4] J.C. Committee, Recommendations for design and construction of high performance fiber reinforced cement composites with multiple fine cracks, Japan Society of Civil Engineers, Tokyo, Japan (2008).
- [5] S. Cahier Technique, Béton fibré ultra-performant (BFUP)-Matériaux, dimensionnement et exécution, Projet (2014).
- [6] F. Baby, B. Graybeal, P. Marchand, F. Toutlemonde, UHPFRC tensile behavior characterization: inverse analysis of four-point bending test results, Materials and structures 46 (2013) 1337-1354.
- [7] S.-C. Lee, H.-B. Kim, C. Joh, Inverse Analysis of UHPFRC Beams with a Notch to Evaluate Tensile Behavior, Advances in Materials Science and Engineering 2017 (2017).
- [8] J.Á. López, P. Serna, J. Navarro-Gregori, E. Camacho, An inverse analysis method based on deflection to curvature transformation to determine the tensile properties of UHPFRC, Materials and Structures 48 (2015) 3703-3718.
- [9] J.A. López Martínez, Characterisation of The Tensile Behaviour of UHPFRC by Means of Four-Point Bending Tests, 2017.
- [10] M. Khorami, J. Navarro-Gregori, P. Serna, M. Navarro-Laguada, A testing method for studying the serviceability behavior of reinforced UHPFRC tensile ties, IOP Conference Series: Materials Science and Engineering, IOP Publishing, 2019, pp. 012022.
- [11] P.H. Bischoff, Tension stiffening and cracking of steel fiber-reinforced concrete, Journal of materials in civil engineering 15 (2003) 174-182.
- [12] J. López, P. Serna, J. Navarro-Gregori, H. Coll, Comparison between inverse analysis procedure results and experimental measurements obtained from UHPFRC Four-Point Bending Tests, Proceedings of the 7th RILEM Workshop on High Performance Fiber Reinforced Cement Composites (HPFRCC7), 2015, pp. 185-192.
- [13] P.H. Bischoff, Effects of shrinkage on tension stiffening and cracking in reinforced concrete, Canadian Journal of Civil Engineering 28 (2001) 363-374.